Cureus Journal of Engineering
https://doi.org/10.7759/s44388-025-00042-x

Original Article

Hydrothermal Synthesis of 3-Dimensional Graphene Foam

Deepali Parag Butala [1], Shobha A. Waghmode [2], Pradnya Giri [2]

1. *Department of Chemistry, Sir Parashurambhau College (Autonomous), Pune, IND*
2. *Department of Chemistry, MES Abasaheb Garware College, Pune, IND*

Received: September 15, 2025 | Review began: January 18, 2026 | Review ended: February 28, 2026 | Published: March 30, 2026

Abstract

Three-dimensional (3D) graphene foam has emerged as a promising material due to its interconnected porous network, large surface area, functional versatility, and many other unique properties being discovered day by day. In the present study, template-free synthesis for the fabrication of 3D graphene foam was experimented with using graphene oxide prepared via the modified Hummers method. Among the two template-free approaches, hydrothermal synthesis and freeze-casting synthesis, particular emphasis was placed on the hydrothermal route owing to its simplicity, cost-effective apparatus, and scalability. Aqueous graphene oxide dispersions were subjected to hydrothermal treatment, enabling the simultaneous reduction and self-assembly of graphene sheets into a stable three-dimensional porous framework without the use of any external templates. The structural and chemical characteristics of the hydrothermally synthesized graphene foam were systematically analyzed using Fourier Transform Infrared spectroscopy, Raman spectroscopy, and Field Emission Scanning Electron Microscopy, which confirm the formation of an interconnected 3D graphene network. Moreover, the graphene foam prepared in this way exhibited notable antimicrobial activity, owing to its unique morphology and surface functionalities, which are discussed in detail in the article. The results explain that template-free hydrothermal synthesis is an effective, quicker and environmentally benign approach for producing 3D graphene foam, highlighting its potential for antimicrobial and many other functional applications.

Categories: Advanced Materials, Materials Engineering, Nanotechnology

Keywords: template-free synthesis, porous graphene network, antimicrobial activity, 3 dimensional graphene foam, hydrothermal synthesis, raman spectroscopy, fesem

Introduction

Graphene is studied all over the world because of its properties, like its flexible two-dimensional structure, single-atom thickness, and exceptional physical and chemical properties. Graphene and chemically modified graphene can be applied to various technological fields like field effect devices, energy storage materials, electrocatalysis, sensors, among others. Self-assembly is considered to be the best strategy for bottom-up nanotechnology. With its unique structure and properties, graphene is a versatile nanoscale building block for self-assembly to get new structures and functionalities. Recent work has shown that multiple stages are required for the self-assembly of graphene films into high-performance thin films and strong, layered, paper-like materials. However, the mechanism in the self-assembly of two-dimensional graphene sheets into three-dimensional macrostructures still needs to be studied for the synthesis of graphene materials with industrial importance.

In this paper, we have explained the synthesis of high-performance self-assembled graphene hydrogel (SGH) via a one-step hydrothermal method [1]. Carbon is used as a raw material for various industrial processes, and its production from various bio-resources is under research. Environmental disasters, energy scarcity, and consumer requirements have made

it necessary to look for environmentally friendly, simple, non-toxic, and low-cost methods for the synthesis of useful carbon materials that can be applied for large-scale production in the future [2]. Recently, carbon spheres have gained interest because of the porous nature of the spheres, high electrical conductivity, and chemical stability, with applications in different fields like catalysis, supercapacitors, and adsorbents. Different methods like template-assisted chemical vapor deposition and hydrothermal carbonization treatment can be used for the preparation of carbon spheres. Among these methods, hydrothermal carbonization treatment is more useful for its controlled carbon sphere size and mild operational conditions. Therefore, the hydrothermal process is a practical and effective method for the synthesis of carbon particles at low pressure and temperature [3-6]. The hydrothermal process has gained importance due to its benefits in the synthesis of nano-structural materials with applications in wide areas like ceramics, catalysis, magnetic data storage, optoelectronics, and electronics. The hydrothermal technique, along with the production of mono-dispersed and highly homogeneous nanoparticles, helps in the processing of nano-composite and nano-hybrid materials. The term "hydrothermal" is of geological origin. The term was first applied by Sir Roderick Murchison, the British geologist, to describe the action of water at elevated pressure and temperature in changing the earth's crust, leading to the formation of a variety of minerals and rocks. The largest crystal created in nature is the beryl crystal (weighing more than 1000 g), and the large quantity of single crystals formed by man, e.g., quartz crystal (weighing more than 1000 g) in one experiment are both of hydrothermal origin [7-9].

Among various techniques available for the processing of advanced materials, the hydrothermal technique occupies a unique place because of its advantages over other conventional techniques [10,11]. The hydrothermal processing of advanced materials is advantageous and is used to obtain high purity of the product, crystal symmetry, homogeneity, narrow particle size distributions, metastable compounds with unique properties, and a wide range of chemical compositions [12,13]. The other advantages of the technique are lower sintering temperature, lower energy requirements, the lowest residence time, single-step processes, sub-micron to nanoparticles with a narrow size distribution using simple equipment, fast reaction times, the growth of crystals with polymorphic modifications and low to ultra-low solubility, and a variety of other applications [14-16]. The reaction in which a mixture of solute and solvent is kept in the autoclave and allowed to react at a controlled temperature for the generation of autogenous pressure, and a product is obtained, is known as a hydrothermal reaction. Materials with aligned porosity in the micrometre range are of technological importance in fields like electronics, microfluids, nanowires, and biomaterials [17].

The development of three-dimensional graphene foam (3DGF) is the field of attraction, as its interconnected porous network provides high surface area, excellent electrical conductivity, and advantageous mass-transport pathways for catalytic, sensing, and energy applications [18]. The use of hydrothermal methods to fabricate such 3D graphene frameworks and to combine them with functional nanostructures offers a straightforward route to well-controlled morphology, crystallinity, and hybrid integration [19].

Hydrothermal synthesis provides a unique autonomous environment of higher temperature and pressure in a closed aqueous system, which promotes the nucleation and growth of highly crystalline nanostructures, often with tunable size, shape, and composition [20]. For graphene foam, the hydrothermal process serves both purposes: the reduction of graphene oxide (GO) and the self-assembly of the 3DG network, while simultaneously enabling the growth or incorporation of graphene functional materials, if intended, within the foam skeleton [20,21].

For example, Luo et al. incorporated graphene quantum dots (GQDs) into a 3D graphene foam via a one-step hydrothermal treatment of GQDs and GO; the resulting GQDs/3DG composites showed improved capacitance relative to pure 3DG [22]. Similarly, Jia et al. reported a one-pot hydrothermal approach for the synthesis of Gd-doped TiO_2 on a reduced graphene oxide (rGO) support, yielding a "3D flower-like" Gd/TiO_2@rGO composite with an increased visible-light photocatalytic effect [23,24].

In this work, we have presented the hydrothermal synthesis of 3DGF designed for antimicrobial application. The novelty lies in new architecture control and a green synthesis route. We systematically investigate the resultant morphology and structure using X-ray diffraction, Field Emission Scanning Electron Microscopy, and Raman, maintaining identical external parameters and the performance of the material in the antimicrobial application.

Materials And Methods

Materials and methodology

Materials

Graphite powder, graphene oxide (prepared by modified Hummers method), GOk (prepared by modified Hummers method using potassium dioxide), strutted graphene, deionized water, Teflon cup, and stainless steel autoclave.

Synthesis

Synthesis of 3DGF was carried out in two main steps.

Preparation of Graphite Oxide by Modified Hummer's Method: In brief, the graphite oxide was prepared by adopting a modified Hummers method from graphite powder. To the mixture of 1 g graphite powder and 1 g sodium nitrate, 23 ml of cooled conc. sulphuric acid was added. Three grams of potassium permanganate were added slowly and gradually by maintaining the temperature below 20 °C. Stirring was continued at a temperature of 35 °C. Water (46 ml) was slowly added to reach 98°C, and the mixture was maintained at that temperature for half an hour. The reaction was terminated by the addition of more distilled water and 10 ml of 30% hydrogen peroxide solution. A solid product was obtained by centrifugation followed by three repeated washings of 5% hydrochloric acid followed by three washings of distilled water to remove acid. The product graphite oxide was dried at 65°C in an oven overnight (Product a.1 Table *1*).

Preparation of Three-Dimensional Graphene by Hydrothermal Method: A colloidal dispersion of GO was prepared by mixing the fixed quantity of graphite oxide with water, followed by ultrasonication. This colloidal dispersion of graphene oxide was subjected to hydrothermal reaction at 130°C for 48 hours. After 48 hours, the autoclave is removed from the oven and allowed to cool naturally to room temperature. Then the autoclave is unsealed and the product is collected.

Product Code	Carbon Source
a.1	Graphene oxide (GOh)
a.2	Strutted graphene
a.3	Graphene oxide (GOk)

TABLE 1: Reactants used in hydrothermal reaction

For the preparation of the remaining products, an identical scheme is followed. The GO was substituted by other reactants like GOk and strutted graphene. This graphitic material was dispersed in 50 ml of water by sonication for 1 hour each. The colloidal dispersion was transferred to a Teflon cup and placed in a stainless steel autoclave. Then it is sealed properly and kept in the oven at 130 °C for 48 hours. The product obtained is first washed with acetone, followed by water, and then dried in the oven at 70°C.

How to cite this article:
Butala D, Waghmode S A, Giri P (March 30, 2026) Hydrothermal Synthesis of 3-Dimensional Graphene Foam. Cureus J Eng 3 : es44388-025-00042-x. DOI https://doi.org/10.7759/s44388-025-00042-x

Results And Discussion

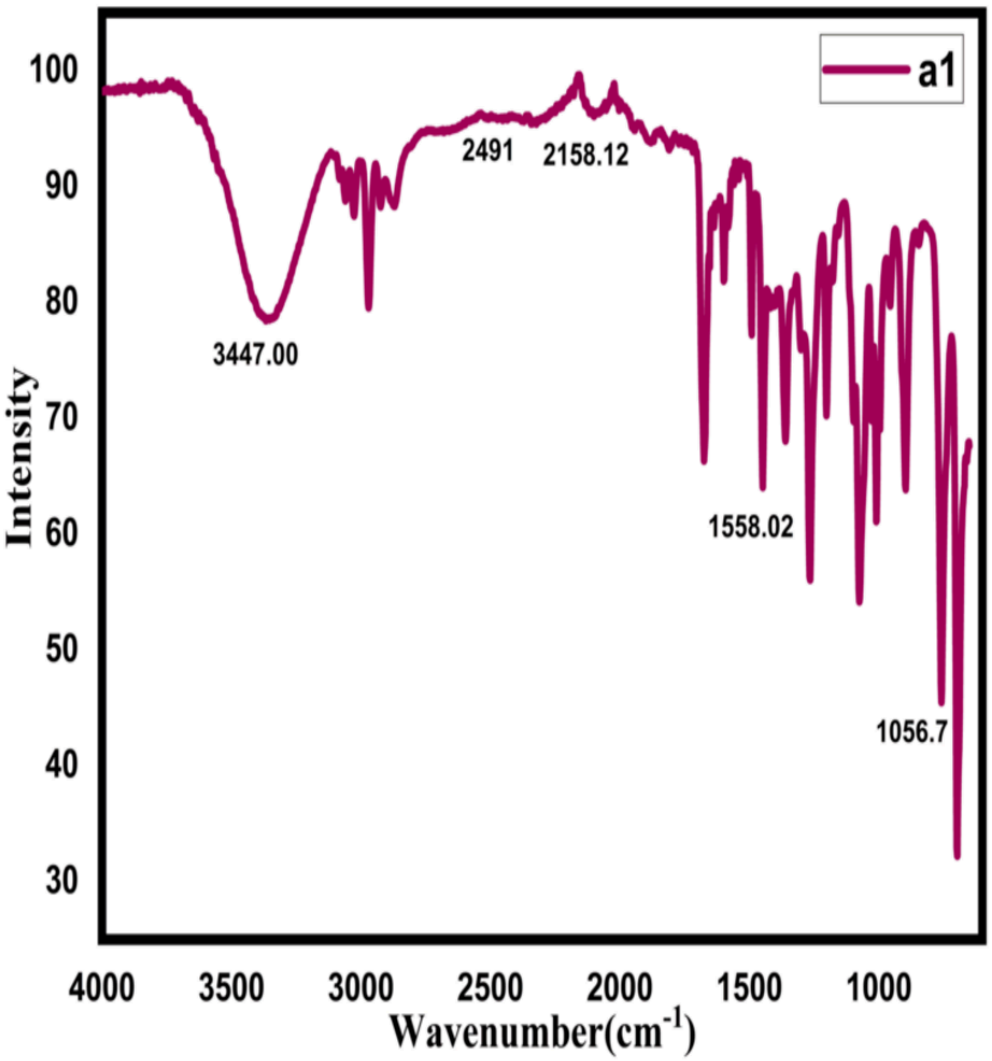

FIGURE 1: FTIR spectra for the product a.1

FTIR, Fourier Transform Infrared Spectroscopy

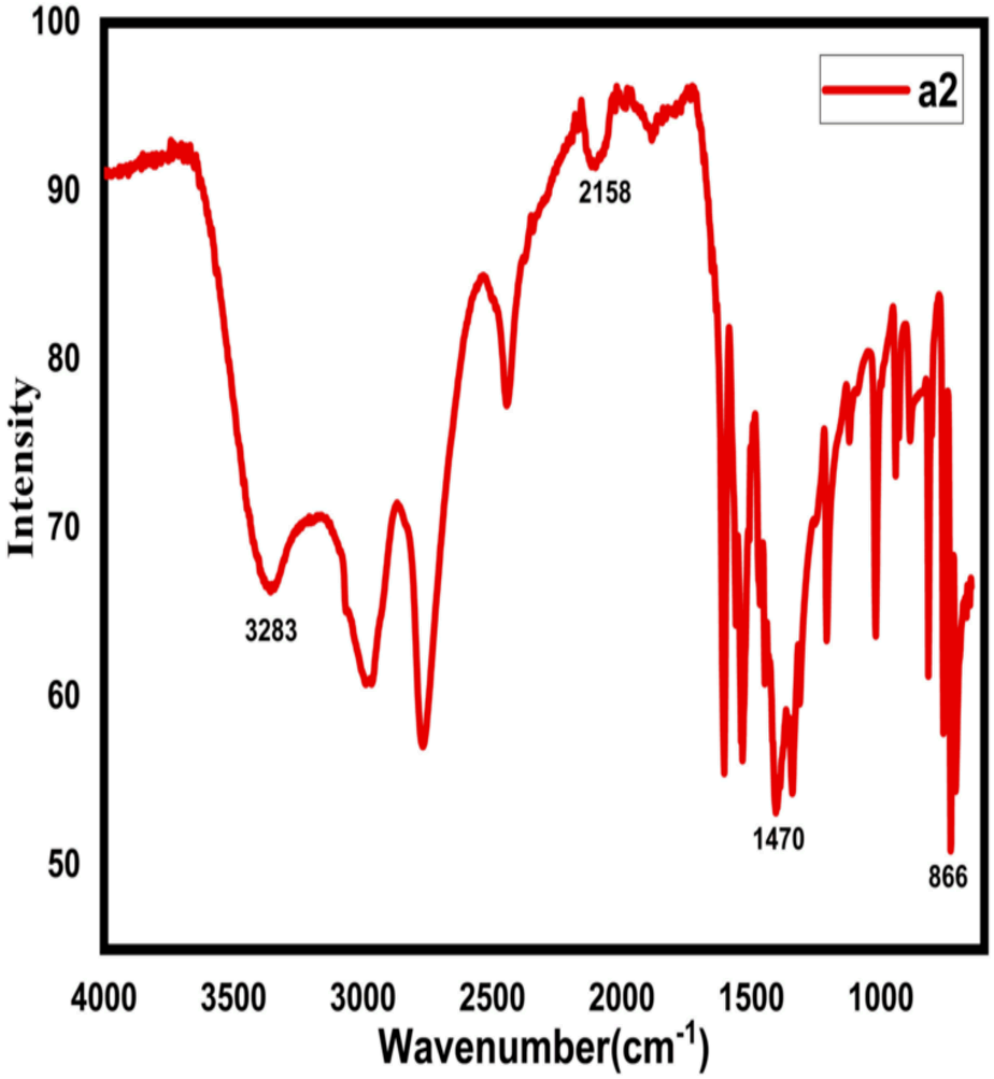

FIGURE 2: FTIR spectra for the product a.2

FTIR, Fourier Transform Infrared Spectroscopy

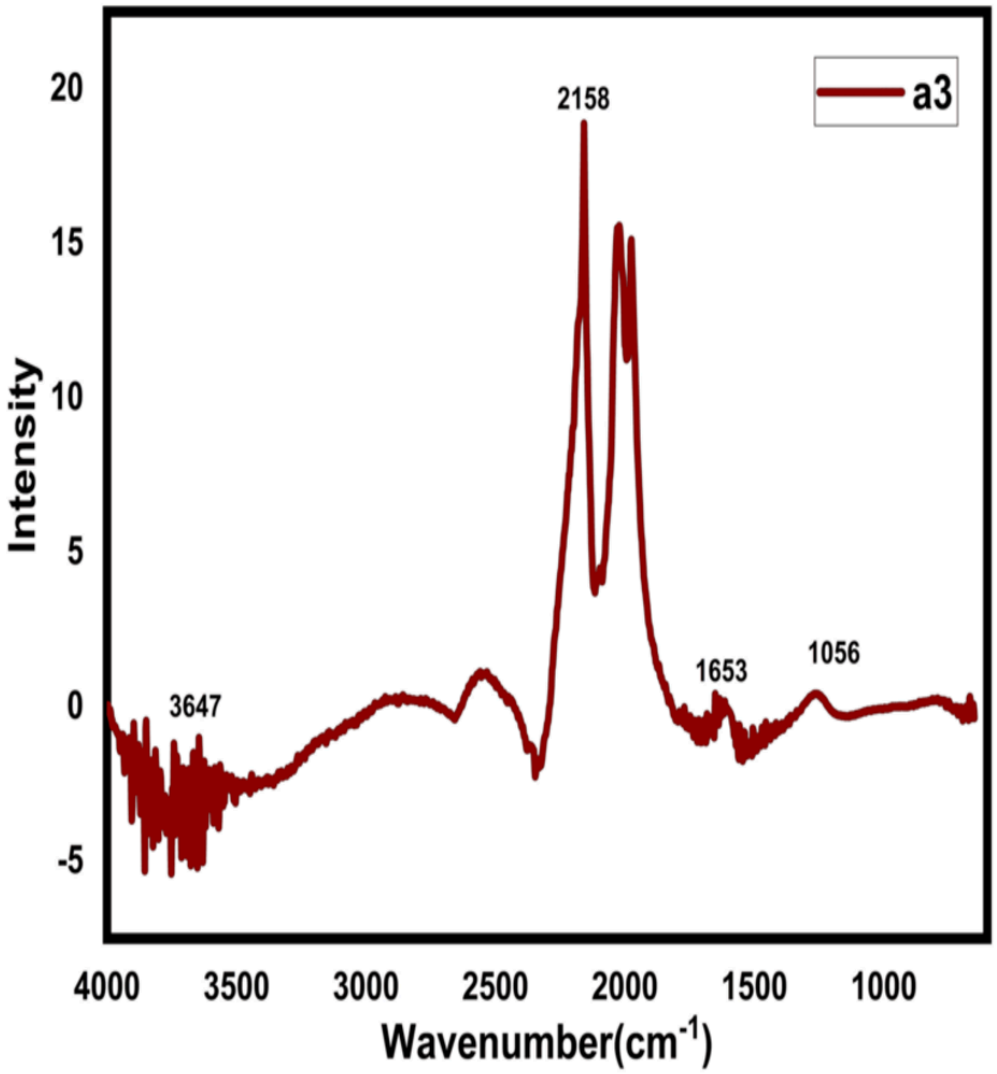

FIGURE 3: FTIR spectra for the product a.3

FTIR, Fourier Transform Infrared Spectroscopy

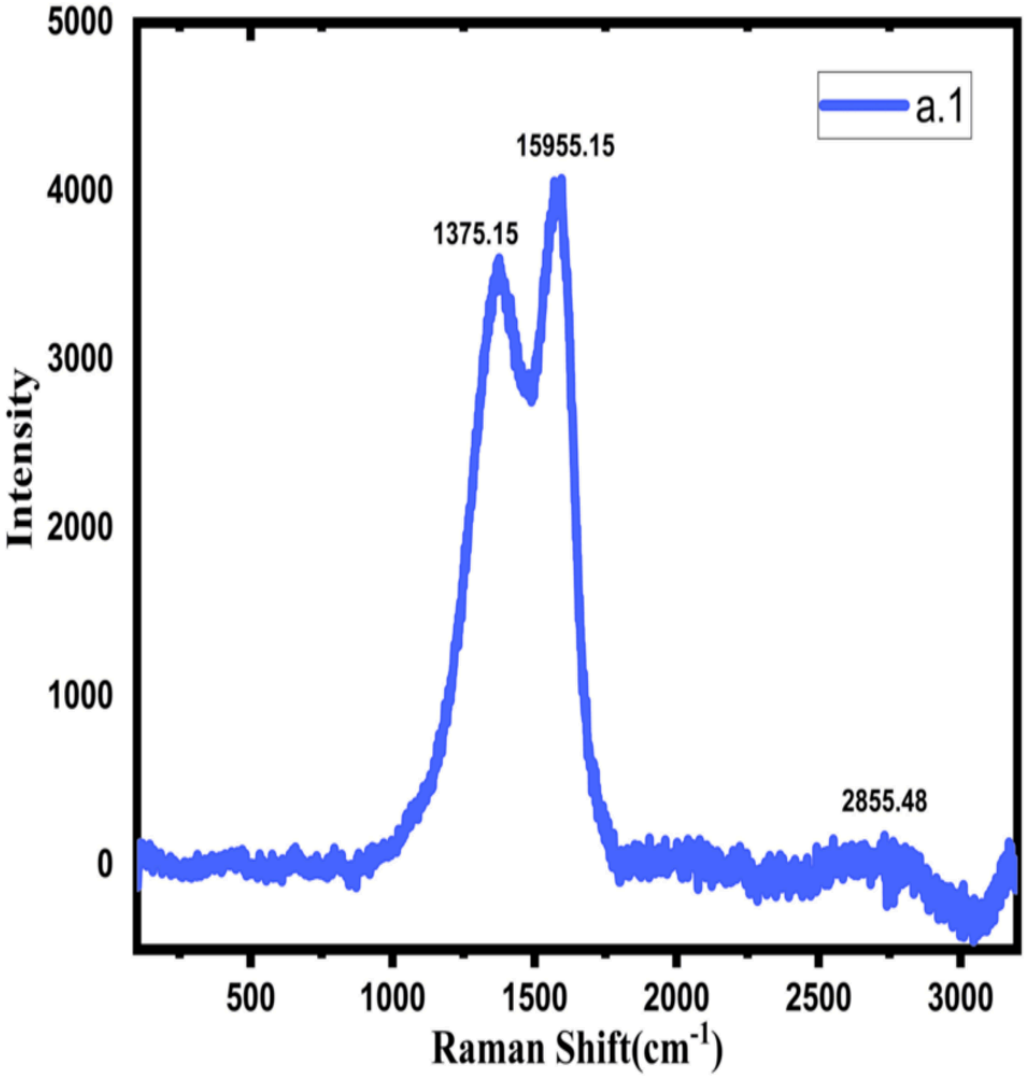

FIGURE 4: Raman spectra for the product a.1

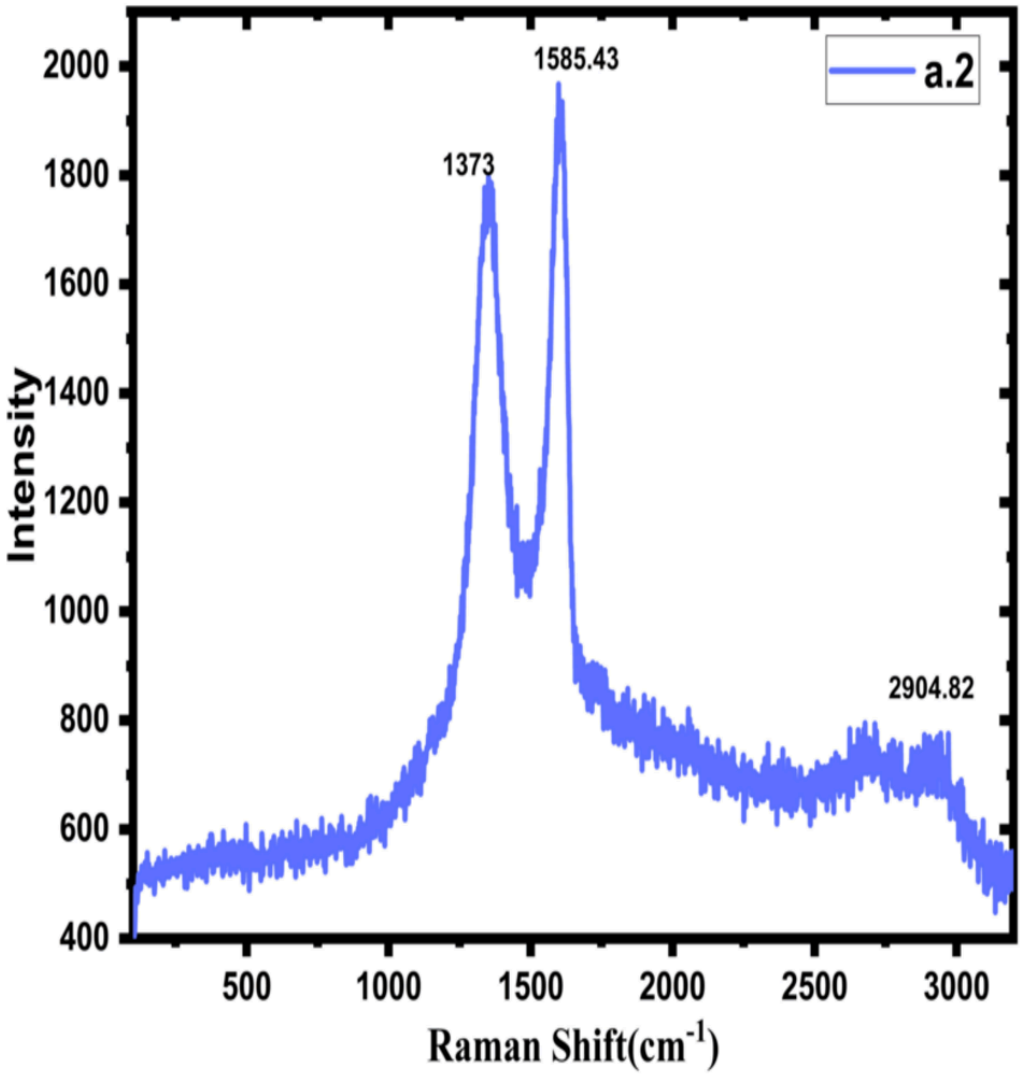

FIGURE 5: Raman spectra for the product a.2

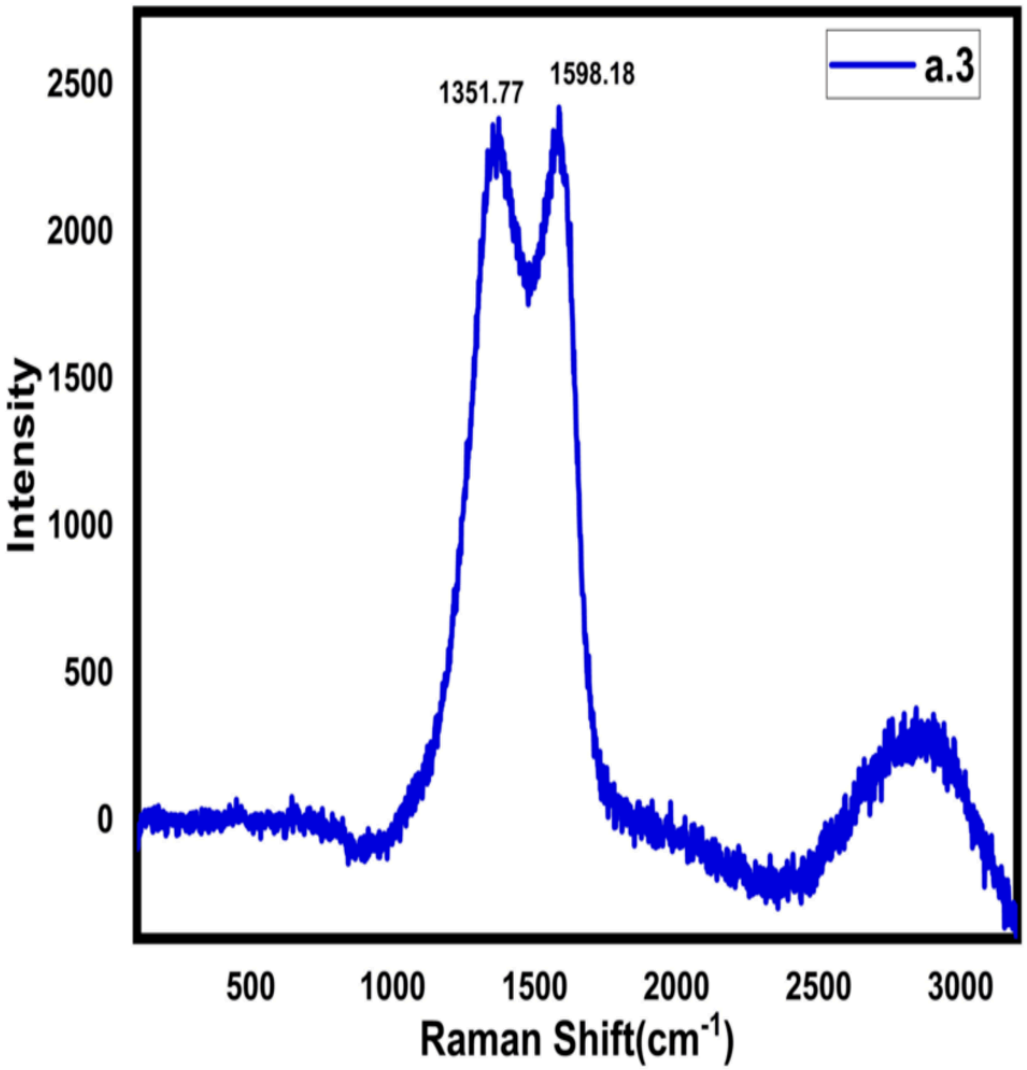

FIGURE 6: Raman spectra for the product a.3

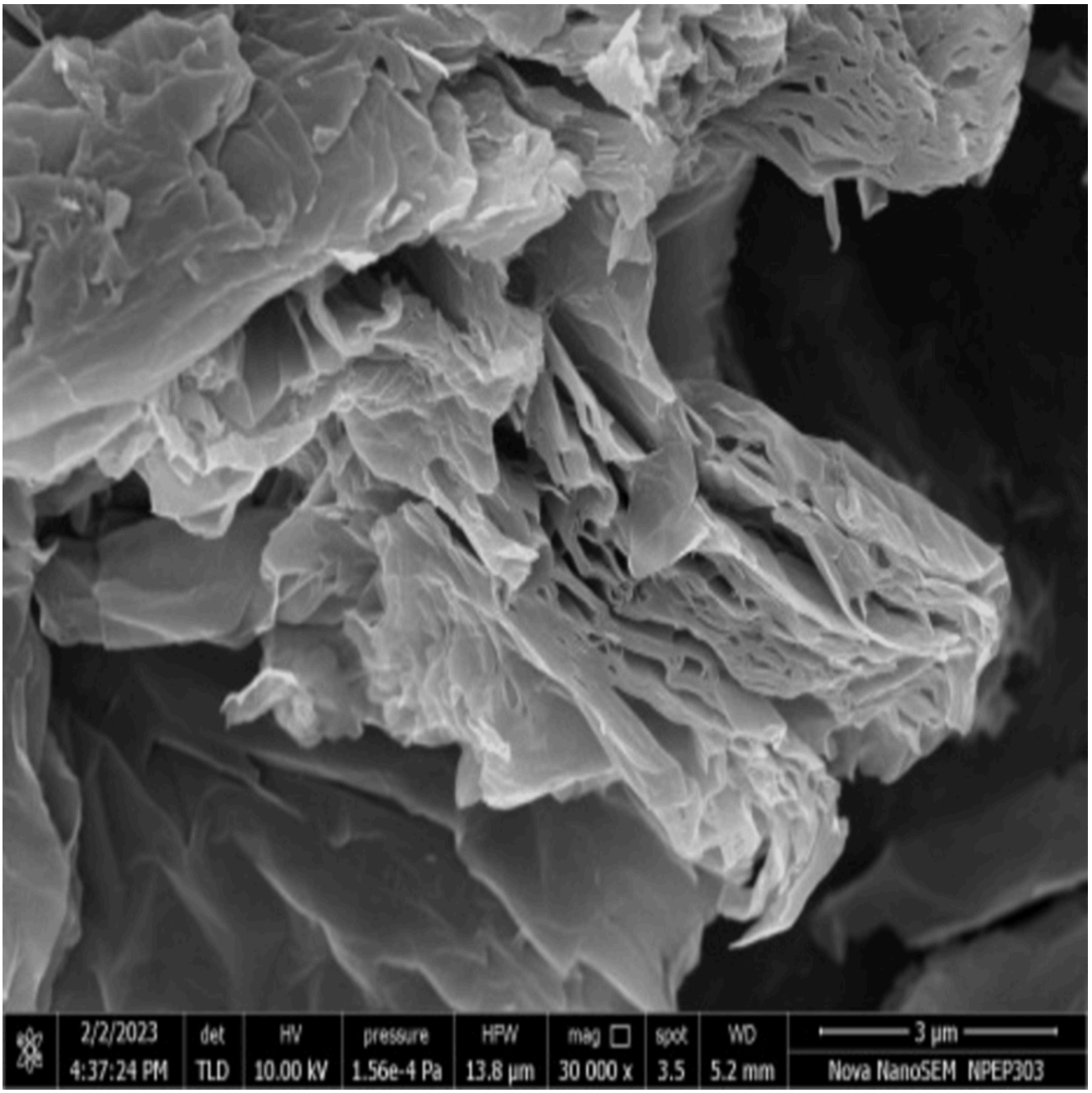

FIGURE 7: FESEM image for the product a.1

FESEM, Field Emission Scanning Electron Microscopy

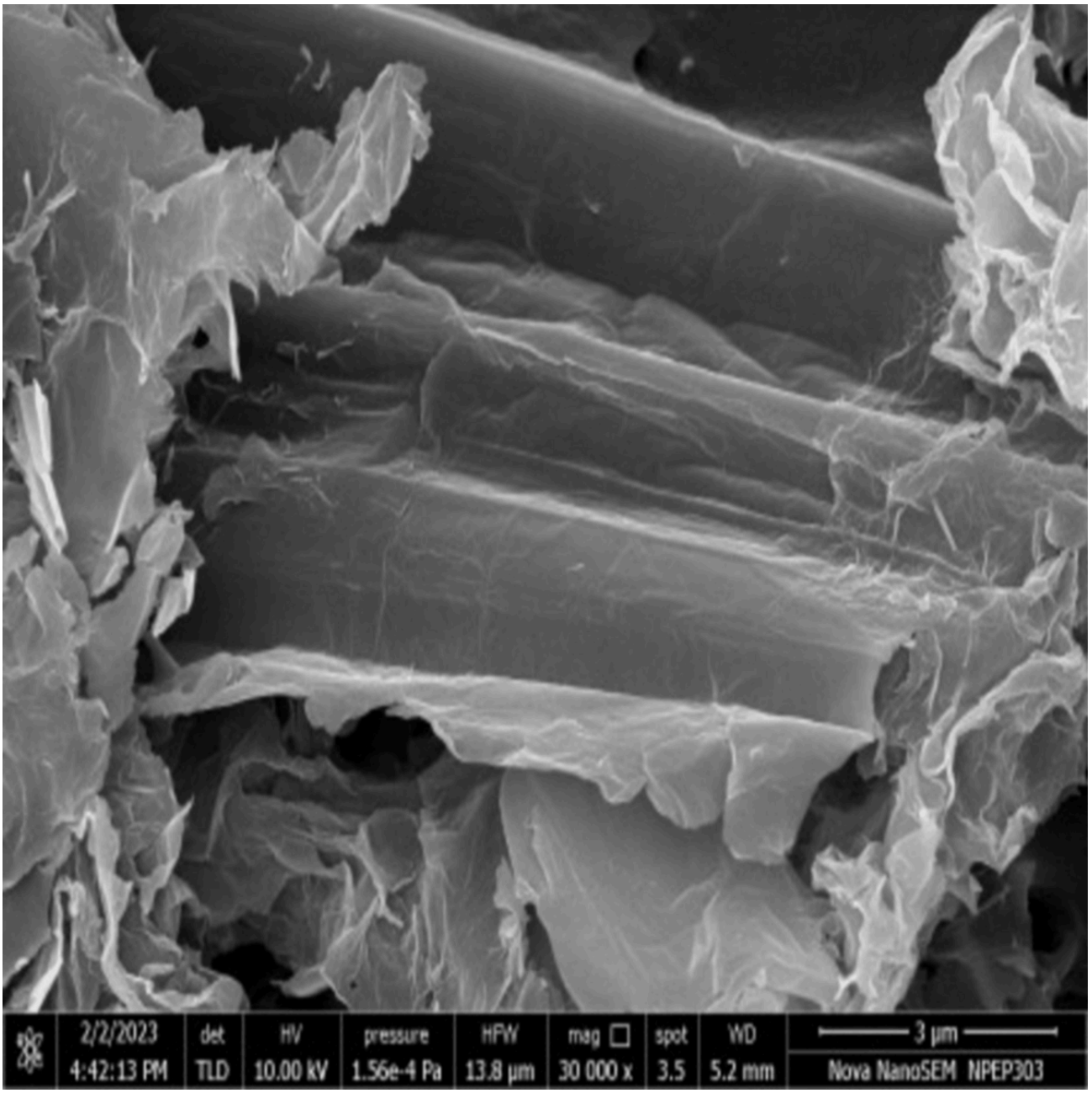

FIGURE 8: FESEM image for the product a.2

FESEM, Field Emission Scanning Electron Microscopy

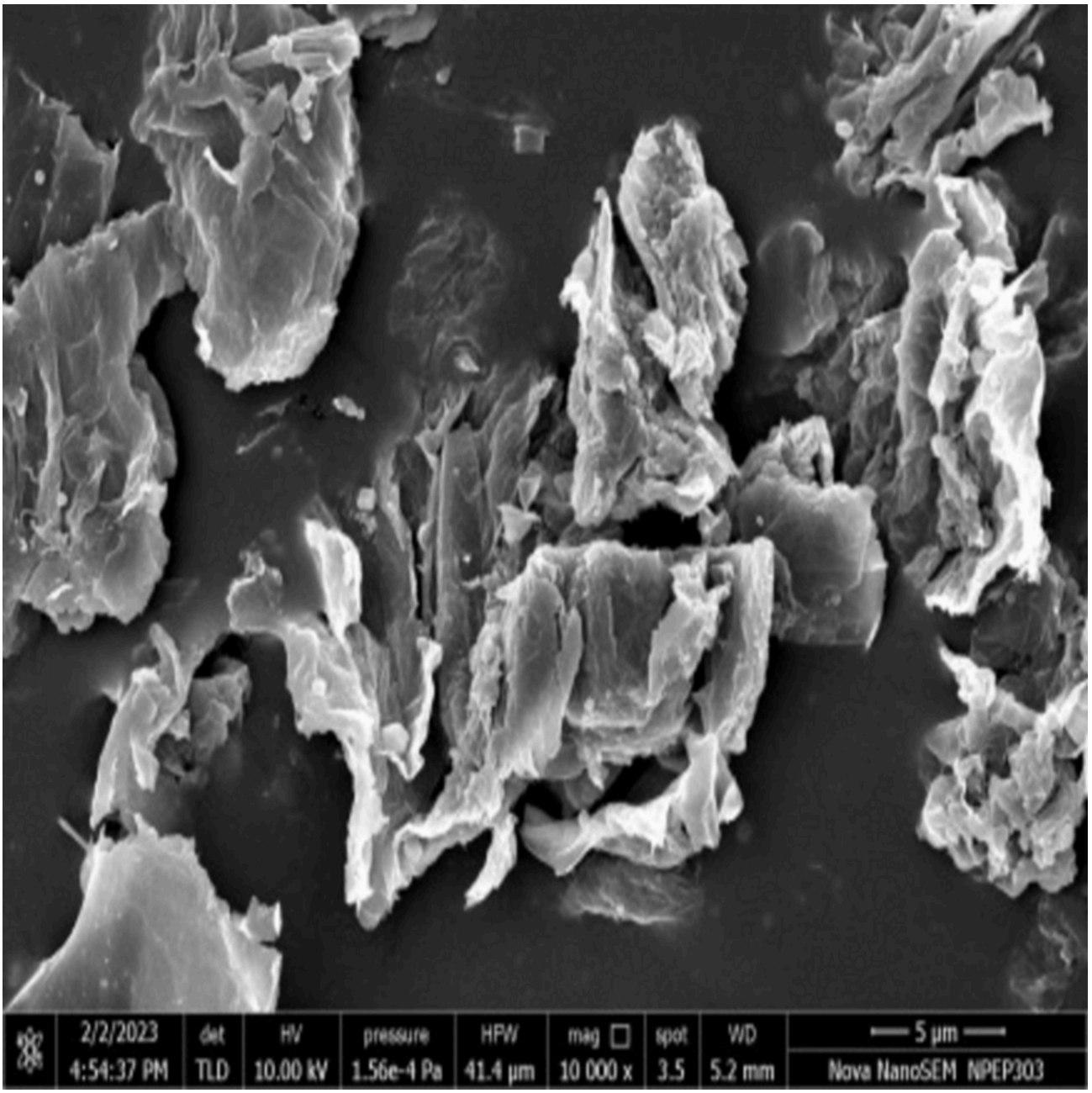

FIGURE 9: FESEM image for the product a.3

FESEM, Field Emission Scanning Electron Microscopy

Discussion

The Fourier Transform Infrared Spectroscopy (FTIR) spectra of graphene (Table *2*) a.1 (Figure *1*) shows the peak at 1056 cm^{-1}.This peak is due to the carbon-oxygen bond in the graphene. The peak at 1558 cm^{-1} corresponds to aromatic C=C stretching. The peak at 2158.12 cm^{-1} corresponds to C=C stretching vibrations, and the peak at 3447 cm^{-1} is due to O-H or C-H stretching. This confirms that the synthesized graphene contains some oxygen functionalities. The FTIR spectra of graphene a.2 (Figure *2*) shows the peak at 866 cm^{-1}, which is due to the bending of the carbon-oxygen (-C=O) bond in the carbonate functionality. The peak at 1470 cm^{-1} corresponds to aromatic C=C stretching. The peak at 2158 corresponds to C=C stretching vibrations, and the peak at 3283 cm^{-1} is due to O-H or C-H stretching. This confirms that

the synthesized graphene contains some oxygen functionalities. The FTIR spectra of graphene a.3 (Figure *3*) shows the peak at 1056 cm^{-1}. This peak is due to the carbon-oxygen bond in the graphene. The peak at 1653 cm^{-1} corresponds to aromatic C=O stretching. The peak at 2158 corresponds to C=C stretching vibrations, and the peak at 3647 cm^{-1} is due to O-H or C-H stretching. This confirms that the synthesized graphene contains some oxygen functionalities. From FTIR analysis, all three graphene samples have peaks in the 1056-866 cm^{-1} region, indicative of C-O or C=O oxygen functionalities. Peaks around 1470-1558 cm^{-1} correspond to aromatic C=C stretching, while the consistent signal at ~2158 cm^{-1} is attributed to C=C stretching vibrations. Broad signals at 3283-3647 cm^{-1} reflect O-H or C-H stretching. These collectively confirm oxygen functionalization, including hydroxyl, carboxyl, or carbonate groups, in all samples. Oxygen-containing functional groups, such as hydroxyls (-OH), carbonyls (C=O), and epoxides (C-O-C), from the graphene oxide introduce sites that can generate reactive oxygen species (ROS). When GO adheres to microbial membranes, ROS like superoxide and hydroxyl radicals are formed, which may damage proteins, lipids, and DNA. This has been observed across various bacterial strains and is an important contributor to antimicrobial effect. There can be ROS-independent oxidative stress via electron transfer like GO acting as an electron acceptor, pulling electrons from microbial membranes leading to disruption of redox homeostasis. This electron transfer results into oxidative stress and eventually cell death. FTIR data, showing oxygen functional groups in all three graphene samples (a.1, a.2, a.3), thus assures the presence of active sites significant for these redox-based interactions.

In Raman spectra (Table *3*) of graphene a.1 (Figure *4*), there are three peaks at 1375.15, 1595.15, and 2855.48. The peak at 1375.15 cm^{-1} is the D peak due to the defects or disorder in the graphene lattice. The peak at 1595.15 is a G peak corresponding to the E2g phonon mode. It arises from the in-plane vibrational motion of sp2-bonded carbon atoms, and the peak at 2855.48 is the G' band (or 2D double-resonance band). In Raman spectra of graphene a.2 (Figure *5*), three peaks at 1373, 1585.15, and 2904.48 correspond to the D peak, G peak, and G' peaks, respectively. The peak at 1373 cm^{-1} is the D peak due to the defects or disorder in the graphene lattice. The peak at 1585.15 cm^{-1} is a G peak corresponding to the E2g phonon mode. It arises from the in-plane vibrational motion of sp2-bonded carbon atoms, and the peak at 2904.48 cm^{-1} is the G' band (Or 2D double-resonance band). In Raman spectra of graphene a.3 (Figure *6*), the two peaks at 1351.77 and 1598.18 correspond to the D peak and G peak, respectively. The peak at 1351.77 cm^{-1} is the D peak due to the defects or disorder in the graphene lattice. The peak at 1598.18 is a G peak corresponding to the E2g phonon mode. It arises from the in-plane vibrational motion of sp2-bonded carbon atoms. Raman spectra reveals the D and G bands (e.g., D ~ 1350-1385 cm^{-1}, G ~ 1575-1600 cm^{-1}) in the samples a.1, a.2, a.3, The D bands reflect lattice defects and disorder. The G bands indicate sp^2-hybridized carbon structures. Defects, such as vacancies, edge sites, or topological irregularities, play dual roles: anchoring functional groups and supporting ROS generation and electron transfer, enhancing reactivity and antimicrobial potency [25,26].

FESEM images (Figure *7*) of the graphene a.1 shows an accordion-like 3D structure with pores at the edges and confirms the presence of micro-channels formed by interconnected flakes forming micro-channels and also reveals the exfoliated structure of 3D graphene. FESEM images (Figure *8*) of the graphene a.2 shows crumpled sheets of graphene in a discontinuous manner which provide increased surface area and physical trapping. FESEM of the graphene a.3 (Figure *9*) shows a highly porous graphene structure with the diameter of the pores in the range of 900-1200 nm consisting of discontinuous crumpled sheets. Porous and crumpled structures enhance contact with microbes, enriching adsorption and mechanical disruption. These open architectures facilitate access and improve interactions with oxygen functional groups and defect-rich areas. All structures thus exhibit a highly porous network with pore diameters of 900-1200 nm, supporting microbe-material interactions.

Application

Antimicrobial Application

The antibacterial activity of the graphene prepared was tested against the two Gram-positive bacteria, two Gram-negative bacteria, and the two fungi by the well diffusion method (Kirby-Bauer test, imaged in Figure *10*). In brief, approximately 20 ml of sterile molten nutrient agar broth was poured into the Petri plates and allowed to solidify on cooling. A 10 mg/ml sample was loaded into the wells. Raman analysis of the products provides data confirming the

presence of the D band (~1350-1385 cm^{-1}) across samples, indicating structural defects or disorder in the graphene lattice. The G band (~1585-1598 cm^{-1}) consistently demonstrates high sp^2 carbon network order from in-plane π bonding. Samples a.1 and a.2 exhibit a clear G′ (2D) band (~2855-2904 cm^{-1}), suggesting few-layer or turbostratic graphene stacking, whereas a.3 lacks a distinct 2D peak, indicating different layer arrangements or higher defect density.

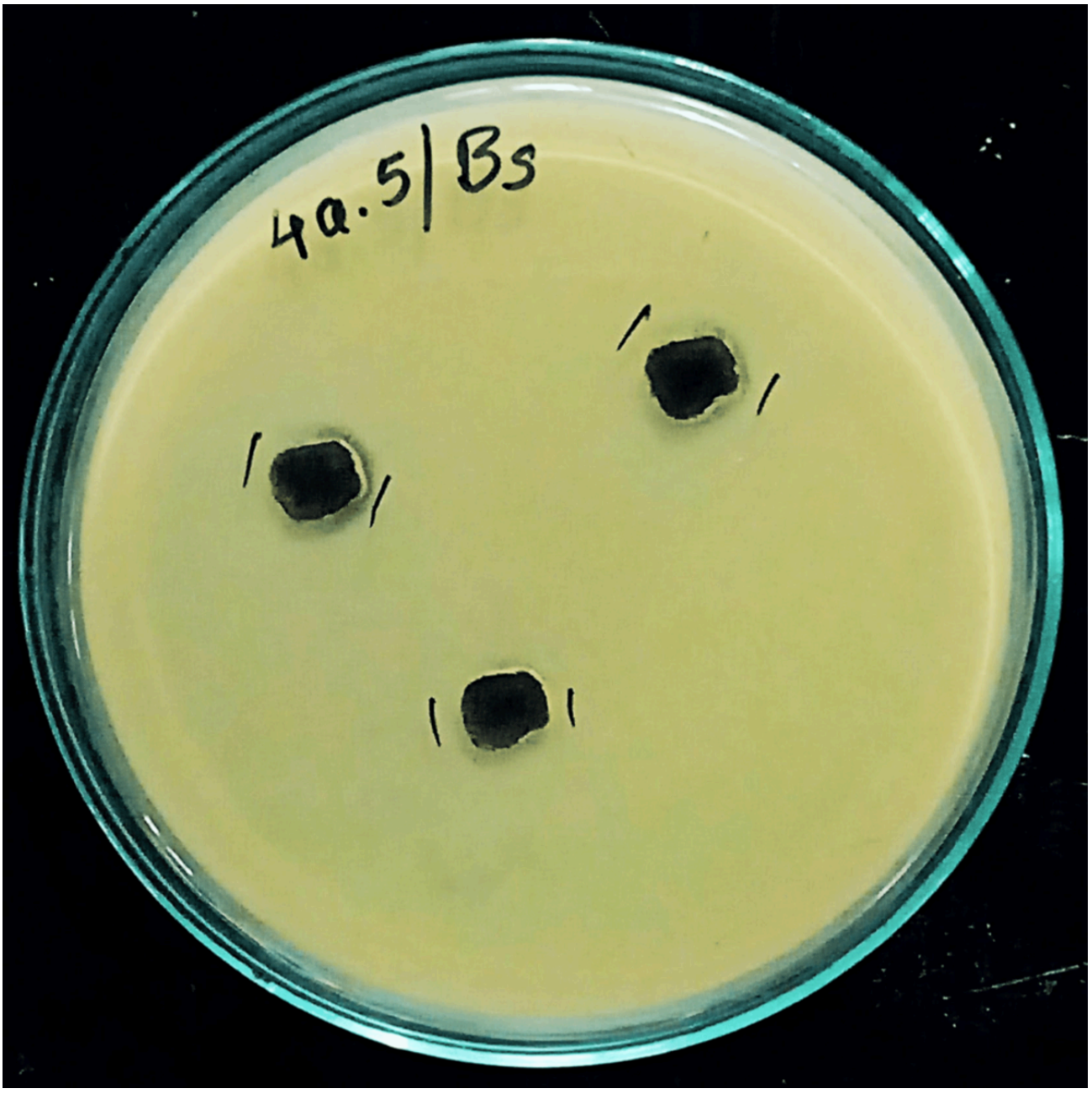

FIGURE 10: Antimicrobial activity image KIrby-Bauer method

The zone of inhibition data:a.2: strong zones (~18-19 mm against *Candida albicans* and *Aspergillus niger*; ~12 mm for *Escherichia coli*); a.3: slightly lower (~17 mm vs *Candida*). These differences reveal variations in oxygen functionalization types (e.g., carbonate in a.2 vs carbonyl in a.3) or differences in defect density or distribution and differences in structural

morphology impacting microbe-material interaction. The graphene shows better antifungal activity than the graphene for the fungi *A. niger* and *C. albicans* and also exhibits better antibacterial activity for the bacteria *E. coli* and *Staphylococcus aureus*.

Product Name	FTIR Values
a.1	1056.7, 1558.02, 2158.12, 2491, 3447.00
a.2	866, 1470, 2158,3283.
a.3	1056, 1653, 2158, 3647.

TABLE 2: FTIR values of graphene synthesized by hydrothermal method

FTIR, Fourier Transform Infrared Spectroscopy

Product Name	D peak	G peak	2D peak
a.1	1375.15	1595.15	2855.48
a.2	1373	1585.43	2904.33
a.3	1351.77	1598.18	

TABLE 3: Raman spectra of Graphene synthesized by hydrothermal method

Conclusions

The combined spectroscopic and microscopic analysis confirms that the hydrothermally graphene samples incorporate oxygen-containing functional groups and exhibit typical sp^2 carbon lattice signatures, along with distinct structural morphologies. All graphene samples demonstrated notable antibacterial and antifungal activity in Kirby-Bauer assays. Graphene exhibited stronger antifungal efficacy against *A. niger* and *C. albicans* and superior antibacterial effects against *E. coli* and *S. aureus* compared to control or unmodified graphene. Successful synthesis and characterization of these products was carried out in the research along with antimicrobial application. Specific surface area and porosity is provided by the hydrothermal method. GO and GOk give better 3D morphology than the strutted graphenes. The graphene a.2 shows better antifungal activity than the graphene a. 3 for the fungi *A. niger* and *C. albicans*.

Additional Information

Author Contributions

All authors have reviewed the final version to be published and agreed to be accountable for all aspects of the work.

Concept and design: Deepali Parag Butala, Shobha A. Waghmode

Acquisition, analysis, or interpretation of data: Deepali Parag Butala, Shobha A. Waghmode, Pradnya Giri

Drafting of the manuscript: Deepali Parag Butala, Shobha A. Waghmode, Pradnya Giri

Critical review of the manuscript for important intellectual content: Deepali Parag Butala, Pradnya Giri

Supervision: Deepali Parag Butala, Shobha A. Waghmode

Disclosures

Human subjects: All authors have confirmed that this study did not involve human participants or tissue. **Animal subjects:** All authors have confirmed that this study did not involve animal subjects or tissue. **Conflicts of interest:** In compliance with the ICMJE uniform disclosure form, all authors declare the following: **Payment/services info:** Rashtriya Uchchatar Shiksha Samiti (RUSA, S. P. College) has provided the funding for the autoclave, along with the Teflon cup required for the hydrothermal reaction during this research work. The Central Instrumentation Facility (CIF), Department of Chemistry, SPPU, Pune, provided us with the FESEM facility. The Department of Physics, SPPU, provided us with Raman characterization. The Department of Chemistry at S. P. College provided FTIR characterization data, and the antimicrobial activity was conducted at Shikshan Prasarak Mandali's Prof. B. V. Bhide Foundation for Research, Innovation, and Incubation. . **Financial relationships:** All authors have declared that they have no financial relationships at present or within the previous three years with any organizations that might have an interest in the submitted work. **Other relationships:** All authors have declared that there are no other relationships or activities that could appear to have influenced the submitted work.

Data Availability Statements

The datasets (and/or code) supporting this study are available from the corresponding author upon reasonable request.

Acknowledgements

This article was previously presented at the International Conference on Next Generation Technology in Science and Engineering (ICNGTSE 2025) at Pranveer Singh Institute of Technology, Kanpur (PSIT) on 22nd–23rd August 2025." The corresponding author and other authors are thankful to Dr. T. R. Ingle Research Laboratory, Department of Chemistry, Sir Parashuramhau College (Empowered Autonomous), Tilak Road, Pune, for making the infrastructure and the required facilities available during the work. Also, the authors are thankful to the Department of Chemistry, Sir Parashuramhau College (Empowered Autonomous), Tilak Road, Pune, and the Department of Chemistry, MES Abasaheb Garware College (Autonomous), Karve Road, Pune. The authors are also thankful to Rashtriya Uchchhatar Shiksha Samiti (RUSA) for funding the necessary equipment for the experiments.

References

1. Xu Y, Sheng K, Li C, Shi G: Self-assembled graphene hydrogel via a one-step hydrothermal process. ACS Nano. 2010, 4:4324-4330. 10.1021/nn101187z
2. Khan TA, Saud AS, Jamari SS, Rahim MHA, Park JW, Kim HJ: Hydrothermal carbonization of lignocellulosic biomass for carbon rich material preparation: A review. Biomass and Bioenergy. 2019, 130:105384. 10.1016/j.biombioe.2019.105384
3. Byrappa K, Adschiri T: Hydrothermal technology for nanotechnology. Progress in Crystal Growth and Characterization of Materials. 2007, 53:117-166. 10.1016/j.pcrysgrow.2007.04.001
4. Titirici MM, Antonietti M: Chemistry and materials options of sustainable carbon materials made by hydrothermal carbonization. Chemical Society Reviews. 2010, 39:103-116. 10.1039/b819318p
5. Baccile N, Laurent G, Babonneau F, Fayon F, Titirici MM, Antonietti M: Structural characterization of hydrothermal carbon spheres by advanced solid-state MAS 13C NMR investigations. The Journal of Physical Chemistry C. 2009, 113:9644-9654. 10.1021/jp901582x

6. Yao C, Shin Y, Wang LQ, et al.: Hydrothermal dehydration of aqueous fructose solutions in a closed system. The Journal of Physical Chemistry C. 2007, 111:15141-15145. 10.1021/jp074188l

7. Krishnamurthy G, Namitha R: Synthesis of structurally novel carbon micro/ nanospheres by low temperature-hydrothermal process. Journal of the Chilean Chemical Society. 2013, 58:1930-1933. 10.4067/s0717-97072013000300030

8. Vijay MV, Butala D, Waghmode S: Carbon Quantum Dots. Research & Reviews in Biotechnology & Biosciences. 2021, 8:101-107. 10.5281/zenodo.5775437

9. Qiu L, Liu JZ, Chang SLY, Wu Y, Li D: Biomimetic superelastic graphene-based cellular monoliths. Nature Communications. 2012, 3:1241. 10.1038/ncomms2251

10. Butala DP, Waghmode SA: Graphene foam: next generation graphene analogue. Research Journal of Chemistry and Environment. 2020, 24:178-188.

11. Vickery JL, Patil AJ, Mann S: Fabrication of graphene-polymer nanocomposites with higher-order three-dimensional architectures. Advanced Materials. 2009, 21:2180-2184. 10.1002/adma.200803606

12. Deville S: Freeze-casting of porous biomaterials: structure, properties and opportunities. Materials. 2010, 3:1913-1927. 10.3390/ma3031913

13. Wu ZS, Winter A, Chen L, Sun Y, Turchanin A, Feng X, Müllen K: Three-dimensional nitrogen and boron co-doped graphene for high-performance all-solid-state supercapacitors. Advanced Materials. 2012, 24:5130-5135. 10.1002/adma.201201948

14. Tang Z, Shen S, Zhuang J, Wang X: Noble-metal-promoted three-dimensional macroassembly of single-layered graphene oxide. Angewandte Chemie. 2010, 122:4707-4711. 10.1002/ange.201000270

15. Jiang X, Ma Y, Li J, Fan Q, Huang W: Self-assembly of reduced graphene oxide into three-dimensional architecture by divalent ion linkage. The Journal of Physical Chemistry C. 2010, 114:22462-22465. 10.1021/jp108081g

16. Li C, Shi G: Functional gels based on chemically modified graphenes. Advanced Materials. 2014, 26:3992-4012. 10.1002/adma.201306104

17. Butala D: Comparative study of antibacterial applications of zinc oxide nanoparticles and polymer nanocomposite. Journal of Engineering and Technological Sciences. 2019, 6:101-105.

18. Nethravathi C, Rajamathi M: Chemically modified graphene sheets produced by the solvothermal reduction of colloidal dispersions of graphite oxide. Carbon. 2008, 46:1994-1998. 10.1016/j.carbon.2008.08.013

19. Geim K, Novoselov KS: The rise of graphene. Nature Materials. 2007, 6:183-191. 10.1038/nmat1849

20. Luo P, Guan X, Yu Y, Li X, Yan F: Hydrothermal synthesis of graphene quantum dots supported on three-dimensional graphene for supercapacitors. Nanomaterials. 2019, 9:201-201. 10.3390/nano9020201

21. Zhang J, Zhu Z, Jiang J, Li H: Ultrasound-assisted hydrothermal fabrication of AgI/MFeO3/g-C3N4 (M = Y, Gd, La) nano sheet-sphere-sheet photocatalysts with enhanced photodegradation activities for norfloxacina. Catalysts. 2020, 10:373. 10.3390/catal10040373

22. Guo L, He Y, Chen D, Du B, Cao W, Lv Y, Ding Z: Hydrothermal synthesis and microwave absorption properties of nickel ferrite/multiwalled carbon nanotubes composites. Coatings. 2021, 11:534. 10.3390/coatings11050534

23. Jia S, Li J, Sui G, Du L, Zhang Y, Zhuang Y, Li B: Synthesis of 3D flower-like structured Gd/TiO2@rGO nanocomposites via a hydrothermal method with enhanced visible-light photocatalytic activity. RSC Advances. 2019, 9:31177-31185. 10.1039/c9ra06045f

24. Waghmode SA, Butala DP: Graphene from Solid Waste Materials for water Purification. The 2-Dimensional World of Graphene. Bentham Science Publishers, Dubai; 2024. 3. 10.2174/9789815238938124010l

25. Pandit B, Agarwal A, Patel P, Sankapal BR: The electrochemical kinetics of cerium selenide nano-pebbles: the design of a device-grade symmetric configured wide-potential flexible solid-state supercapacitor. Nanoscale Advances. 2021, 3:1057-1066. 10.1039/d0na00893a

26. Mendhe AC, Majumder S, Nair N, Sankapal BR: Core-shell cadmium sulphide @ silver sulphide nanowires surface architecture: Design towards photoelectrochemical solar cells. Journal of Colloid and Interface Science. 2021, 587:715-726. 10.1016/j.jcis.2020.11.031